JOURNAL OF MATERIALS SCIENCE 18 (1983) 1405–1420

The influence of morphology and molecular weight on ductile–brittle transitions in linear polyethylene

NORMAN BROWN
Department of Materials Science and Engineering, University of Pennsylvania, Philadelphia, Pennsylvania 18104, USA

I. M. WARD
Department of Physics, University of Leeds, Leeds, UK

The tensile behaviour of linear polyethylene was examined over a wide range of temperatures. Samples were prepared from low and medium molecular weight polymer with different morphologies, by varying the initial crystallization conditions. It was found that the temperature of the ductile–brittle transition was markedly different for different samples. In particular, low molecular weight polymer crystallized at a low degree of of supercooling, showed brittle behaviour over most of the temperature range, with a ductile–brittle transition near to room temperature. Rapidly quenched material, where the degree of supercooling is high, showed a very low ductile–brittle transition temperature, especially in high molecular weight polymer. The reasons for these differences in behaviour are discussed both at a phenomenological level and in terms of known structural differences between the different materials examined.

1. Introduction

There is considerable interest in the fracture behaviour of polyethylene, because of its increasing use in engineering applications such as water and gas pipes. Most of the studies have followed a fracture mechanics approach, and because of the considerable ductility of the material, the fracture tests have generally been conducted either at low temperatures [1] (often with very thick specimens to ensure a plane strain failure mode) or at high ambient hydrostatic pressure [2].

The yield and cold drawing behaviour of polyethylene has also been studied extensively because of the possibility of producing ultra-high modulus oriented polyethylenes in this way [3–6]. In these investigations, the main emphasis has been on the influence of chemical composition, especially molecular weight, and initial morphology on necking and cold-drawing.

The present investigation attempts to estabish the connections between these two lines of research, by determining the factors which influence the ductile–brittle transitions. On the basis of the previous studies, four polyethylene samples have been selected. Low and medium molecular weight polyethylene samples have been prepared with the extreme types of morphology which can be induced by different thermal treatments. It will be shown that there are profound differences in the failure behaviour of different samples. These differences are directly reflected in the ductile–brittle transitions and affect both the ductile and brittle modes of failure. Both notched and unnotched specimens have been examined over a wide range of temperatures.

The results are interpreted in terms of our existing knowledge of the structure of polyethylene, and it will be shown that several features are consistent with contemporary views of the molecular and morphological nature of the different polyethylene structures which have been studied.

0022–2461/83 $03.00 + .12

TABLE I

Material designation	Polymer grade*	Treatment	$\bar{M}_n \times 10^3$	$\bar{M}_w \times 10^3$	Density ($g\,cm^{-3}$)
LSC	Rigidex 50	Slow cooled	6.1	101	0.9725
LQ	Rigidex 50	Quenched	6.1	101	0.9475
HSC	H120/56	Slow cooled	27.8	220	0.9665
HQ	H120/56	Quenched	27.8	220	0.9435

*All polymers were obtained from BP Chemicals.

2. Experimental details

2.1. Preparation of materials

In other investigations in this laboratory [5, 7] the influence of molecular weight and initial thermal treatment on drawing and morphology of linear polyethylene have been examined. Extreme morphologies could be most conveniently produced by direct quenching from the melt or by slow cooling. To establish continuity with this previous work and to enable the work described here to form a rational part of a continuing investigation, we have therefore followed what are now standard procedures in this laboratory for preparing samples of known morphology. The evidence of the previous work also enables us to be selective as to our choice of starting materials. Polymers at two levels of molecular weight were chosen to vary the morphology of the starting materials. Polymer granules or powder were compression moulded into sheets about 0.4 mm thick at $\sim 160^\circ$ C, and then either quenched into water at ambient temperature, or allowed to cool for $\sim 8^\circ\,C\,min^{-1}$ to room temperature. In the case of the low molecular weight material quenching into water leads to a better defined spherulitic structure than does slow cooling. Previous work [5] shows that higher molecular weight material is less affected by thermal treatment. Table I lists the materials, their molecular weights and densities. The densities were measured in a gradient column.

2.2. Mechanical testing procedures

The tensile specimens were about 0.4 mm thick, 4 mm wide with a gauge length of 15 mm. The shoulders had a 12 mm radius of curvature with a low stress concentration so that the brittle specimens generally failed within the region of uniform cross-section. The temperatures of testing ranged from about 313 to 90 K with an uncertainty within $\pm 2^\circ$ C. Temperatures above 313 K were obtained by passing cold nitrogen gas over the specimen. for temperatures below 136 K cold helium was used in order to prevent crazing softening that is produced below 136 K by N_2 as observed by Parrish and Brown [8]. The testing was done with an Instron machine using strain rates from 0.11×10^{-3} to $55 \times 10^{-3}\,sec^{-1}$. The strain was measured from the overall machine displacement minus a correction for the compliance of the machine. The overall uncertainty of the measured stress was about $\pm 3\%$ based on the uncertainty in load and measurements of the cross-sectional area.

3. Results

Three of the polyethylene samples, those labelled LQ, HQ and HSC, undergo a conventional ductile–brittle (D–B) transition at low temperatures in the range 95 to 106 K, as shown in Table II. This transition is marked by a change in the failure mode from localized necking (usually termed necking rupture) to brittle fracture. These two types of failure are illustrated in Figs. 1a and b. The changes in the stress–strain curves during this normal low temperature D–B transition are shown in Fig. 2 where the localized necking prior to fracture produces a pronounced maximum followed by a sharp drop in the stress–strain curve; whereas the brittle fracture occurs in the elastic region. At a phenomenological level of

TABLE II σ_y, σ_F and D–B transition temperatures at $\dot{\epsilon} = 1.1 \times 10^{-3}\,sec^{-1}$

Material	σ_y(MPa) 296 K	σ_F(MPa) 94 K		D–B temp (K)*
LSC	26	101	130–166	260
LQ	18	144	106	243–273
HSC	30	134	116	243–273
HQ	17	152	95	243–273

*See text for descriptions of the four types of D–B transition temperatures.

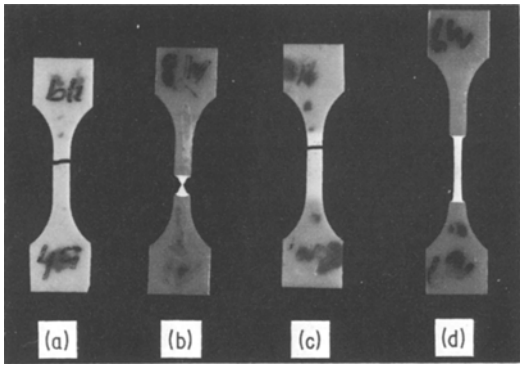

Figure 1 Photographs of the various failure processes. (a) Brittle fracture for all materials. (b) Necking/rupture. (c) Non-necking ductile fracture for the LSC material. (d) Necking/drawing.

interpretation, above the D–B transition temperature, σ_y, the yield stress is less than σ_F, the fracture stress and below the transition temperature vice versa. At this level of explanation, the D–B transition occurs because σ_y increases more rapidly with decreasing temperature than σ_F (see, for example, Ward [9] p. 332 *et seq.*).

The LSC material shows very unusual behaviour in several respects. In the first instance a transition from ductile to brittle behaviour occurs at very high temperatures, but the conventional stress–strain curve for brittle fracture as illustrated in Fig. 2 is only observed following a further transition at low temperatures, close to the D–B transition temperature of the other materials. Fig. 1c shows a typical fractured specimen of LSC material. Fracture occurs with very little change in cross-sectional area between 90 and 300 K. Moreover, the strain prior to fracture is nearly uniform along the gauge length at all temperatures. The stress–strain curves of LSC material are shown in Fig. 3, from which it can be seen that when this material exhibits a yield point, the curvature at the maximum of the stress–strain curve is very small. The sharp drop in the stress at the yield point associated with localized necking, which occurs in all the other materials, is absent.

On the basis of the strain prior to fracture ϵ_F, we have identified two D–B transitions in the LSC material. Fig. 4 shows a plot of ϵ_F against temperature for the LSC material. Between 165 and 260 K, ϵ_F is constant at about 0.065. In this temperature range Fig. 3 shows that the stress–strain curves attain a maximum, but show no drop in stress. Above 260 K, ϵ_F increases rapidly, with the strain being apparently uniform over the gauge length. This is the transition to cold drawing, which we term the upper D–B transition. It is to be particularly noted that, in contrast to the other materials, a sharp neck as shown in Fig. 1d is not observed when cold drawing occurs.

The lower D–B transition for the LSC material begins below 166 K where Fig. 4 shows that ϵ_F gradually decreases with decreasing temperature from 0.065 to 0.038 at about 130 K. Below 130 K, ϵ_F remains approximately constant. Fig. 3 shows that during this low temperature D–B transition, the stress–strain curves gradually fall short of producing a maximum until the curves become almost linear. Under the most brittle condition where $\epsilon_F = 0.038$, the non-linear component of

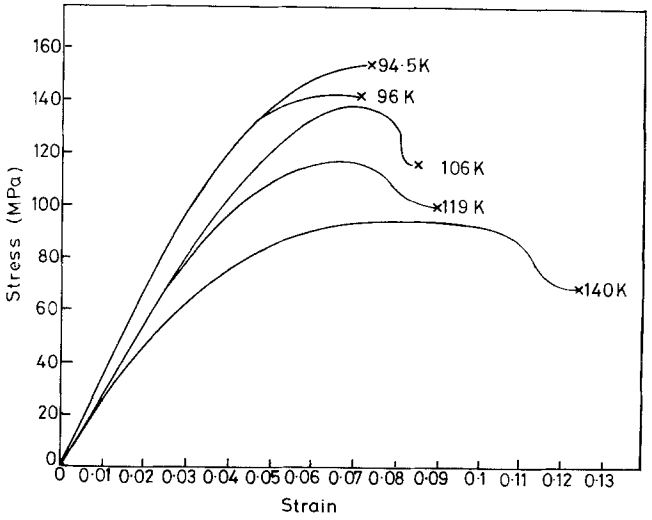

Figure 2 Stress–strain curves at various temperatures for the HQ material showing the low temperature D–B transition. (Strain rate $1.1 \times 10^{-2}\,sec^{-1}$.)

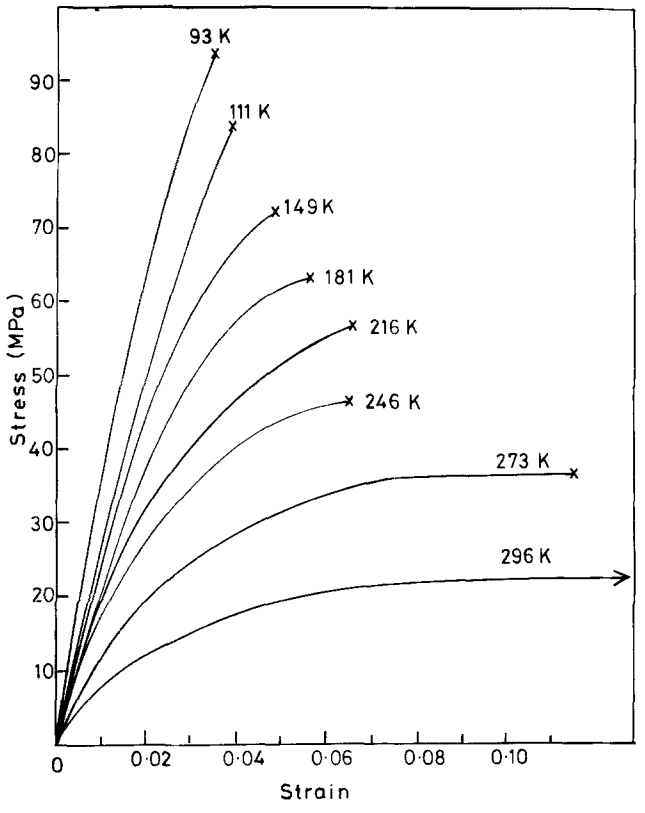

Figure 3 Stress–strain curves for the LSC material from 93 to 296 K. (Strain rate $1.1 \times 10^{-1}\,\mathrm{sec}^{-1}$.)

strain is only about 0.005 and the material is completely elastic up to fracture. We have concluded from all these results that the LSC material undergoes a low temperature D–B transition between 166 and 130 K and a high temperature D–B transition at about 260 K.

The effect of strain rate $\dot{\epsilon}$, on the high temperature D–B transition of the LSC material was investigated. Fig. 4 shows plots of ϵ_F against temperature for two strain rates $\dot{\epsilon} = 1.1 \times 10^{-3}\,\mathrm{sec}^{-1}$ and $\dot{\epsilon} = 22 \times 10^{-3}\,\mathrm{sec}^{-1}$, and Fig. 5 shows plots of ϵ_F against $\dot{\epsilon}$ between 273 and 313 K. It is to be noted that the effect of strain rate on ϵ_F increases with increasing temperature. Below 266 K, $\dot{\epsilon}$ has practically no effect on ϵ_F.

We also investigated the effect of strain rate on the conventional necking rupture/brittle fracture D–B transition exhibited by the LQ, HQ and HSC

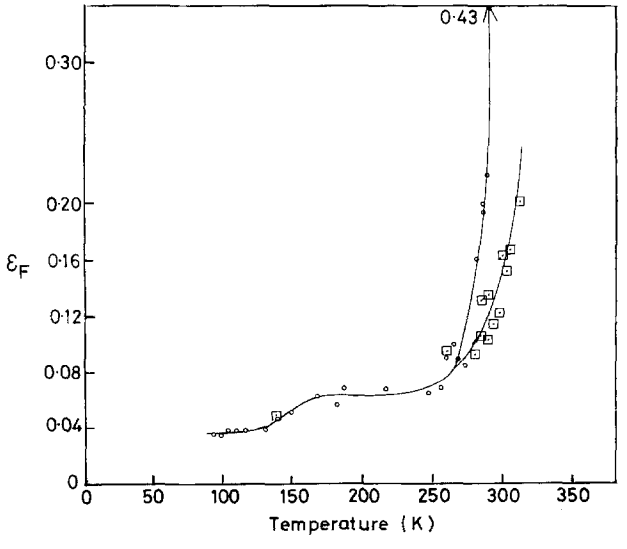

Figure 4 Fracture strain ϵ_F, against temperature for the LSC material at two strain rates: ○, $1.1 \times 10^{-3}\,\mathrm{sec}^{-1}$, ⊡, $2.2 \times 10^{-2}\,\mathrm{sec}^{-1}$.

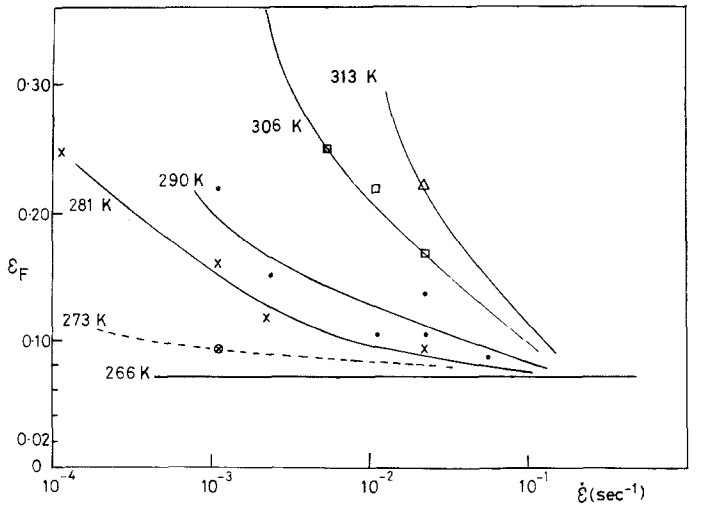

Figure 5 A plot of fracture strain, ϵ_F, against strain rate for the LSC material at various temperatures.

materials. Fig. 6 shows how the stress–strain curves change from localized necking to the brittle fracture mode at 99 K for a range of strain rates from 0.11×10^{-3} to $11 \times 10^{-3}\,sec^{-1}$. It is apparent that the temperature of this D–B transition increases with increasing strain rate.

Particular attention was given to the behaviour of the brittle fracture stress at the lowest temperatures. The effect of strain rates from 1.1×10^{-3} to $55 \times 10^{-3}\,sec^{-1}$ was investigated. It was found that strain rate very slightly increased σ_F, but in all materials σ_F increased with decreasing temperature. Kastelic and Baer [10] found that for PET and PC, $d\sigma_F/dT$ was positive at very low temperatures below 52 and 37 K, respectively. Possibly our temperatures were not low enough to detect this effect.

In the temperature range where the LSC material shows the upper D–B transition from brittle behaviour to cold drawing, the LQ, HQ and HSC materials show the conventional transition from necking/rupture to cold drawing, as illustrated in Fig. 1b and d. In both cases there is a sharp drop in the stress after the maximum, but in one case rupture occurs shortly after the drop in stress whereas in the other case necking is followed by cold drawing. This transition occurs in the temperature range 243 to 273 K. It is emphasized again that the LSC material is different from the other materials in that it does not exhibit a highly localized neck. Any indication of necking which occurs above room temperature is associated with a gradual tapering of the specimen along its gauge length. This feature has been discussed previously by Coates and Ward [6] in the context of the neck shapes in high draw polyethylenes. There may be some objection to calling this transition from necking/rupture to

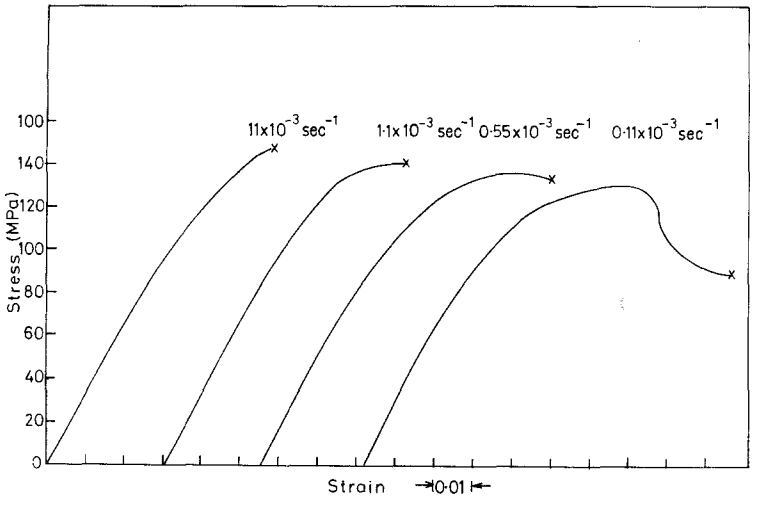

Figure 6 Stress–strain curves at 99 K at various strain rates for the LQ material.

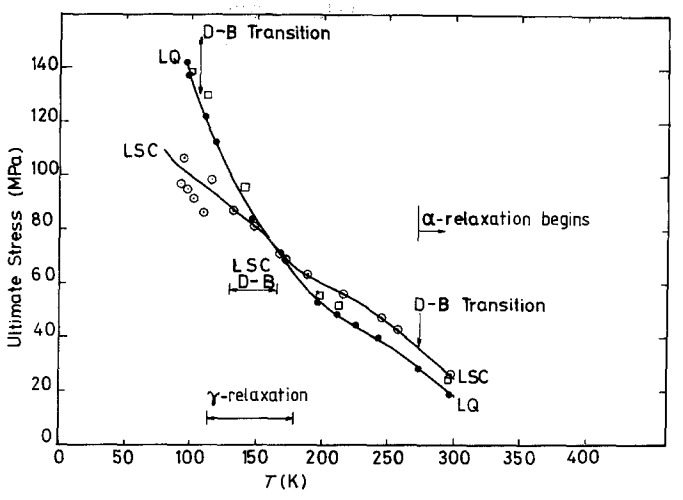

Figure 7 Plot of ultimate stress against temperature for the LQ (•) and LSC (⊙) materials.

necking/cold drawing a D–B transition on the grounds that the localized necking and ductile fracture produces an extremely high localized plastic strain which may be greater than the overall strain in the fully drawn specimen. However, because the average strain after localized necking and fracture is much less than that for a fully drawn and subsequently fractured specimen we consider that it is appropriate to consider that this transition is a D–B transition in a general sense.

In summary then, four D–B transitions have been identified. The temperatures of these transitions are listed in Table II. The LSC material is unique relative to the others and has two D–B transitions, one at 260 K and the other between 130 and 166 K. The LQ, HQ and HSC materials each have a conventional D–B transition ~ 100 K and the necking rupture/cold drawing D–B transition at about 243 to 273 K.

In order to understand the effects of morphology on the D–B transitions, it is important to compare the values of the yield stress, σ_y, and the brittle fracture stress, σ_F, for all the materials. The values of σ_y at 296 K and σ_F at 94 K are given in Table II, and their temperature dependence is shown in Figs. 7 and 8. It can be seen that the ultimate strengths of all the materials, σ_y or σ_F, vary monotonically with temperature. Abrupt changes in slope in the neighbourhood of the D–B transition temperatures are not apparent, although the slope of the σ_F curve tends to be less than that of the σ_y curve in the region of the low temperature D–B transition.

Table II shows that σ_y at 296 K is lower for the slow cooled materials. This result is consistent with a detailed room temperature study [4] of molecular weight and morphology on the yield and drawing behaviour. The yield stress relates primarily to the density (Table I) which is a

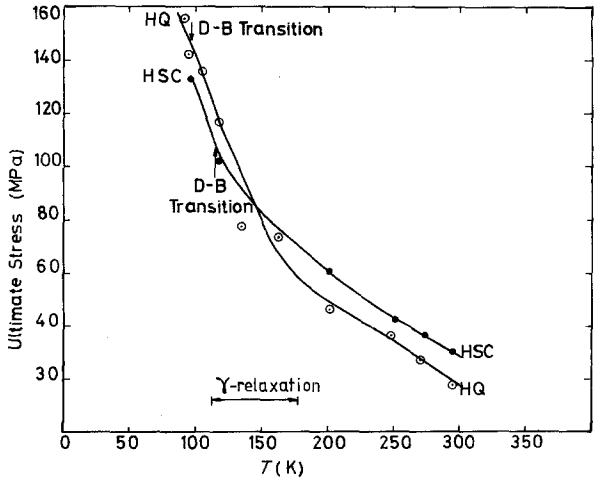

Figure 8 Plot of ultimate stress against temperature for the HQ (⊙) and HSC (•) materials. (Strain rate 1.1×10^{-3} sec^{-1}.)

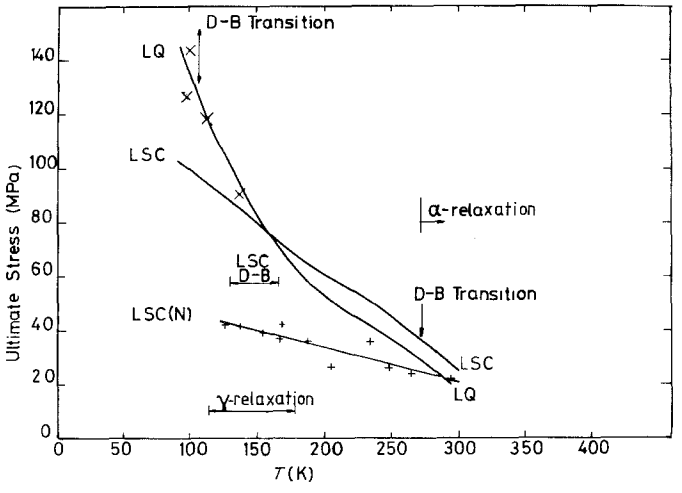

Figure 9 Plot of ultimate stress against temperature for the LSC and LQ materials with and without notches. x shows notch effect in the LQ material.

measure of the crystallinity. In the temperature range where the non-crystalline regions are relatively weak compared with the crystalline regions, differences in σ_y based on differences in crystallinity manifest themselves. It is to be noted from Figs. 7 and 8 that as the temperature is lowered into the region of the γ relaxation, the values of σ_y for all the materials become nearly equal. In the γ relaxation temperature range, the non-crystalline region becomes strong and its yield strength becomes nearly equal to that of the crystals so that differences between the macroscopic yield points of the four materials become small.

We will propose that the differences in brittle fracture stress at 94 K depend primarily on the number of the molecules which hold the crystals together. It is to be expected that the number of tie molecules will increase with molecular weight and be greater for the quenched state. Thus the LSC material has the lowest value of σ_F and the HQ material the greatest. Since σ_y is about the same for all polymers at low temperatures, it is to be expected that the LSC material would have the highest D–B transition temperature and HQ the lowest, based on their relative fracture stresses. Table II shows that this is indeed the case.

The notch sensitivity of the four materials was also investigated. A single-edge notch of length 0.25 mm was inserted at room temperature into the centre of the gauge length edge with a razor blade. The LSC material behaved quite differently from the other three materials with respect to its notch sensitivity. Fig. 9 shows the temperature dependence of the ultimate strength of notched specimens of the LSC material. The curve is practically linear and the difference between notched and unnotched specimens increases with decreasing temperature. For the LQ material, which is representative of the LQ, HQ and HSC materials, the ultimate strengths above 130 K were practically notch-insensitive, but the presence of a notch decreased the failure strain, ϵ_f. For the LSC material the stress–strain curves for the notched specimens were linear to fracture at all temperatures. The other materials were also practically linear to fracture, especially at the lower temperatures.

The notch sensitivties of the LSC and LQ materials are compared in Table III, by making a comparison of the brittle failure stresses for the notched and unnotched specimens (σ_F(N) and σ_F(U), respectively) with the yield stresses of the unnotched specimens (σ_y(U)). It can be seen that

TABLE III Notch sensitivities of the LQ and LSC materials

Material	Temperature (K)					
	296			100		
	σ_F(N) (MPa)	σ_y(U) (MPa)	σ_F(N)/σ_y(U)	σ_F(N) (MPa)	σ_F(U) (MPa)	σ_F(N)/σ_F(U)
LSC	19	26	0.73	47	101	0.47
LQ	18	18	1.0	127	144	0.88

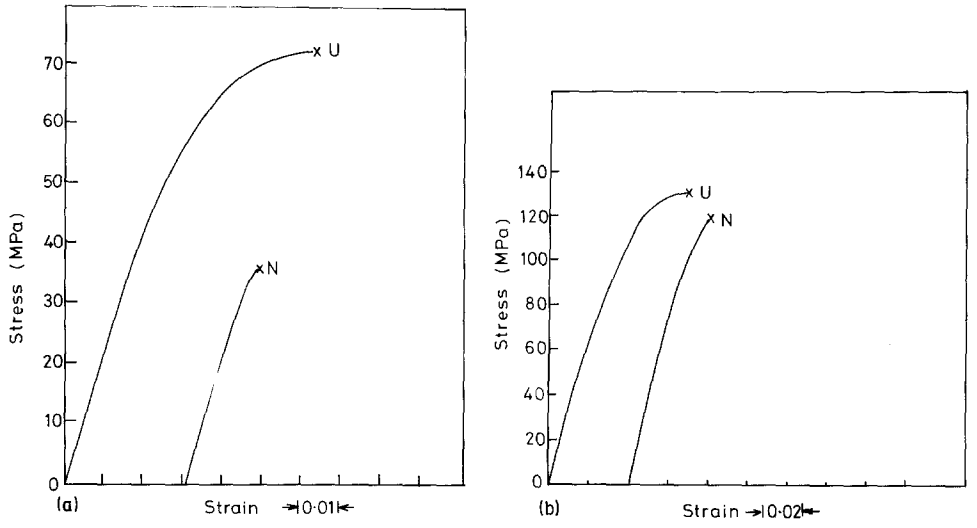

Figure 10 Stress–strain curves with 0.25 mm notch (N) and without a notch (U) for (a) the LSC material at 167 K and a strain rate of $1.1 \times 10^{-3}\,sec^{-1}$, and (b) the LQ material at 113 K and a strain rate of $22 \times 10^{-3}\,sec^{-1}$. Note: ϵ_F is the same for both materials in the unnotched state.

the LQ material is not very notch sensitive even below its brittle temperature, whereas the LSC material is very notch sensitive, especially in its brittle range.

Figs. 10a and b illustrate another aspect of the difference between the notch sensitivity of the LSC material and the other materials. Fig. 10a shows the stress–strain curves for notched and unnotched LSC materials, clearly indicating the large difference in their ultimate strengths. Fig. 10b shows that the LQ material, on the other hand, exhibits very little notch sensitivity. It is of considerable interest to compare Figs. 10a and b, noting that ϵ_F is the same for both materials in the unnotched state (~ 0.06) which indicates similar ductility, yet the LSC material has much greater notch sensitivity. This result is a further indication that the LSC material has a unique structure which is responsible for its unique response to notches as well as its unique D–B transition behaviour.

4. Discussion

4.1. Structural considerations

In order to discuss the relationship between structure and the observed mechanical properties it is useful to consider the differences in structure of the four polyethylene samples. The structures envisaged for these four materials are shown in schematic form in Fig. 11. These diagrams were based primarily on the previous detailed structural studies using small-angle X-ray diffraction, Raman

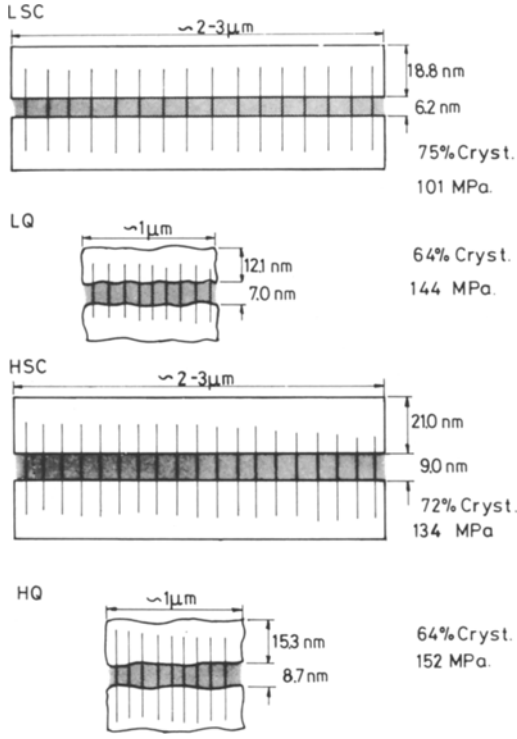

Figure 11 Schematic diagrams of the morphologies of the various materials. Clear area is crystalline; grey area is non-crystalline thickness of each area and is based on data by Capaccio *et al.* [7]. As indicated, the slow cooled materials have sharp interfaces compared to the quenched materials. Vertical dark lines indicate the tie molecules whose spacing is inversely with brittle fracture stress. Note dimensions in thickness directions are not the same scale as for transverse direction. (After Capaccio *et al.* [7] and Bassett *et al.* [12].)

spectroscopy and nitric acid etching [7], but the electron microscope observations of Bassett and Hodge [11] were also helpful in visualizing the morphology.

The schematic diagram of Fig. 11 illustrates the following morphological features which we considered to be relevant for understanding the mechanical behaviour: (1) the amount of amorphous material; (2) the number of tie molecules; and (3) the perfection of the crystals. There are some aspects of the structure which are important for understanding mechanical behaviour but which are not yet amenable to experimental observation. These aspects include the density and slackness of tie molecules, the connections between the tie molecules and the crystals and imperfection in the crystals which cause yielding and their subsequent fragmentation. Such imperfections may lie in the transition region between the so-called amorphous material and the well-ordered crystals. There are also several differences in the lamellar crystals between the slow cooled and quenched materials. In the slow cooled materials the lamellar crystals are both thicker and have greater lateral dimensions. According to Bassett *et al.* [12] the slow cooled materials have widths on the order of about 3 μm compared with about 1 μm for quenched materials. The results of Capaccio *et al.* [7] indicated that the boundary between crystalline and non-crystalline regions was sharper for the slow cooled materials. Bassett and Hodge [11] also showed that the boundaries of material crystallized isothermally at high temperatures (i.e. equivalent to slow cooling, where crystallization also occurs at low degrees of supercooling) are straighter than those for materials crystallized at a greater degree of supercooling (as in quenched materials). All these observations indicate that the slow cooled materials are more perfect than the quenched materials. In general, all crystals grow more perfectly with a decrease in the degree of supercooling.

Not only are the slow cooled crystals more perfect but the total volume of crystalline material (the percentage crystallinity) is greater, as indicated by density and other related parameters [7]. This is shown by the structures in Fig. 11 where the percentage crystallinity is related to the area of the crystalline region relative to the inter-crystalline or amorphous region. We use the term amorphous for the inter-crystalline region with reluctance because amorphous denotes a random, isotropic liquid-like morphology whereas we believe that the inter-crystalline region consists of a variety of structures such as tie molecules with varying degrees of tautness, various types of loose and tie folds, and cilia. There is also a further degree of complexity in that segregated low molecular material in the slow cooled samples might form a second population of thinner lamellae, as shown by the observations of Dlugosz *et al.* [13] and Bassett and Hodge [11].

A central feature of this paper is the proposal that the observed variations in brittle fracture stress relate to the density of tie molecules. The spacing of the tie molecules in Fig. 11 is chosen so that the spacing varies inversely with brittle fracture stress. Although there are no direct observations on the number of tie molecules, there are two types of evidence to support this proposition that differences in the fracture stress of these materials relate to differences in the density of tie molecules.

First, there are the observations of Backman and Devries [14] on the formation of free radicals during the fracture of semi-crystalline polymers. The polymers were cut with a knife and the number of broken covalent bands estimated by electron spin resonance. The number of broken bands observed increased with decreasing temperature until the glass transition temperature. The maximum number of broken bonds per unit area observed was about an order of magnitude less than the number of chains that traverse a unit area of crystal. This result suggested that the fracture line follows a path through the inter-crystalline region because a random cut through the chains within the crystal would yield over ten times more broken chains than were observed. The taut tie molecules offer the best opportunity for being cut. Other molecules could evade the knife by (1) being more mobile, (2) being part of cilia, (3) pulling out of the crystal.

Secondly, the observed brittle fracture values do follow the expected pattern for the concentration of tie molecules, based on our knowledge of the differences in crystallization behaviour. The number of tie molecules is expected to be greater with increasing molecular weight simply because the probability of nucleating a crystal on a given molecule increases with the length of the molecule, Also the number of tie molecules is greater in the quenched material because the

number of nuclei for crystallization increases with the degree of supercooling. That the LQ and HSC materials have about the same brittle fracture stress and presumably the same number of tie molecules is fortuitous in that the two opposing tendencies controlling nucleation happen to balance each other. The important fact is that the kinetics of nucleation of the crystals leads to the LSC material having the smallest number of tie molecules and the HQ material the most.

4.2. Relationship of structure to yield behaviour

The D–B transitions depend on both the yield and fracture behaviour. From a macroscopic viewpoint, the yield stress is defined as the stress that must be exceeded in order to produce a permanent (plastic) strain after unloading. Generally the yield stress is very close to the maximum in the stress–strain curve following the elastic range. The relationship between yield point and structure depends very much on the temperature.

4.2.1 Temperatures between the α- and γ-relaxations

In the temperature range where the non-crystalline region is weak or rubbery and the crystalline region is strong, the degree of crystallinity exerts the primary effect on the yield point. This temperature range extends from above the γ-relaxation, about 180 K, into the α-relaxation range where the crystals begin to soften. The molecular details of the yielding process in semi-crystalline polymers are complex and not completely known (see, for example, a recent review by Haudin [15]) but most models indicate that the stress to produce a permanent strain in the material, the yield point, causes the crystals to be fragmented. There are many detailed speculations of how fragmentation takes place such as those by Peterlin [16]. Peterman *et al.* [17], and Haudin [15], but the general consensus is that the yield point depends on the strength and volume fraction of the lamellar crystals. Since slow cooling increases the crystallinity it is expected that the yield point would increase with crystallinity in this temperature range as has been observed in many other investigations (see, for example, Capaccio and Ward [4]) and simply confirmed here.

It is also suggested that the more perfect crystals produced by slow cooling may be stronger than those produced by quenching. The greater resistance to fragmentation of the more perfect crystals may be associated with the fact that they are thicker as shown in Fig. 11 and are not so easily pulled apart by the molecular network that primarily involves the tie molecules. There is an intimate connection between the pulling by the tie molecules to fragment the crystals and the innate strength or shear resistance of the crystals.

The interlamellar material deforms prior to and during the fragmentation of the crystals and therefore contributes greatly to the strain up to the yield point. When the shear resistance of the non-crystalline region is small compared with that of the crystals, it does not contribute significantly to the yield stress. Thus the yield point depends primarily on the volume fraction of crystals and their strength.

4.2.2. Temperature range where the non-crystalline region is strong

As the material is cooled into the γ-relaxation range, the non-crystalline region becomes rigid so that its strength approaches that of the crystalline region. Consequently the effect of the proportion of crystallinity tends to disappear. As can be observed in Figs. 7 and 8, the yield points of all the polymers become nearly equal below the γ peak at about 170 K. This is a general effect. Kamei and Brown [18] found that branched low density PE and short branched copolymers of PE had yield points at 170 K which were about the same as those observed for the linear polyethylenes in this investigation. (The low density PE value was a little less.) Thus, for PE the yield point below about 170 K is insensitive to structure. The absolute value of the yield point depends on the molecular structure and factors such as the strength of the van der Waals' bonds but not on the details of the morphology.

4.3. Fracture behaviour

4.3.1. Tie molecules

Many aspects of the D–B transitions can be explained on the basis that brittle fracture occurs when the yield point exceeds the fracture stress in accord with the now classical theory as expounded by Ludwig, Davidenkov, Orowan ([9] p. 332) as illustrated in Fig. 12. The D–B transition temperature occurs where the curve of σ_y against T intersects that of σ_f against T. All theories of brittle fracture indicate that σ_f is less sensitive to

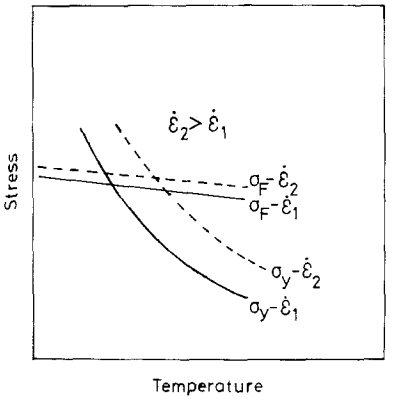

Figure 12 Schematic diagram of fracture stress, σ_f, and yield point, σ_y, plotted against temperature to illustrate that the D–B transition temperature occurs at intersection of σ_y and σ_f curves for a given rate $\dot{\varepsilon}$.

T and $\dot{\varepsilon}$ than σ_y. Thus the D–B transition temperature increases with $\dot{\varepsilon}$ as shown in Fig. 6.

We propose that brittle fracture is caused by bond rupture taking place in the elastic region before crystal fragmentation or plastic shear occurs. The number of tie molecules is expected to be an important factor that determines the variations in fracture stress because the stress to fracture a unit area of covalent bonds is about forty times the stress to fracture a unit area of van der Waals' bonds. This estimate is based on the premise that the fracture stress is proportional to Young's modulus. Thus, the relative values of σ_f for the four materials should increase with the number of tie molecules per unit area. As discussed previously, the number of tie molecules increases with the degree of supercooling and the length of the molecules, as does the fracture stress.

Although the fracture stress increases with the number of tie molecules, a not insignificant part of the fracture stress is associated with breaking van der Waals' bonds. In the absence of tie molecules it is expected that the brittle fracture stress would be given by:

$$\sigma_F = \frac{1}{C}\sigma_{vw} = \frac{1}{C}\beta E_{iso}$$

where C is the stress concentration and σ_{vw} is the ideal strength of the van der Waals' bonds. The ideal fracture stress of all solids is proportional to Young's modulus. Following Kelly [19], the constant of proportionality, β, is about 0.1 to 0.2. E_{iso} is the Young's modulus for the van der Waals' bonds and corresponds to E for isotropic PE which is 8 GPa at 90 K. If $C = 20 - 50$ then $\sigma_F = 0.016 - 0.08$ GPa. Much smaller values of C would give values of σ_F which exceed the observed value of 0.101 GPa for LSC. Much larger values of C do not seem likely without having rather long cracks. Now the fraction of tie molecules can be estimated using the above values of C.

The model assumes that the fracture stress is equal to the sum of the strength of the tie molecules and of the van der Waals' bonds in the interlamellar area.

$$\sigma_f = \frac{1}{C}[f_T \cdot \sigma_T + (1 - f_T)\sigma_{vw}],$$

where C is the stress concentration; f_T is the fraction of the interlamellar area covered by tie molecules (covalent bonds) and σ_T and σ_{vw} are the ideal stresses for the tie molecules and the van der Waals' bonds, respectively.

We then have

$$\sigma_f = \frac{1}{C} f_t \beta E_T + (1 - f_T)\beta E_{iso},$$

where E_T is the Young's modulus of the tie molecules, and has been given the value 300 GPa [20].

Solving for f_T,

$$f_T = \frac{C\sigma_F - \beta E_{iso}}{\beta(E_T - E_{iso})}$$

The results shown in Table IV were then obtained for the materials with extreme fracture stresses. For illustrative purposes we show calculated values of f_T for $\beta = 0.1$ or 0.2 and $C = 20$ or 50. These results agree quite well with the experiments of Backman and Devries [14] who found $f_T = 0.05$ at 243 K. We would expect higher values of f_T at 95 K where our fracture data were obtained. These calculations suggest that the fraction of tie molecules in the HQ material is about twice that in the LSC material. These estimates of tie molecule concentration may be useful in the light of the fact that there

TABLE IV Area fraction of tie molecules f_T calculated from the brittle fracture stress σ_f for the LSC and HQ materials

β	C	f_T	
		LSC material ($\sigma_f = 0.101$ GPa)	HQ material ($\sigma_f = 0.152$ GPa)
0.1	20	0.041	0.075
0.1	50	0.14	0.23
0.2	20	0.007	0.024
0.2	50	0.058	0.100

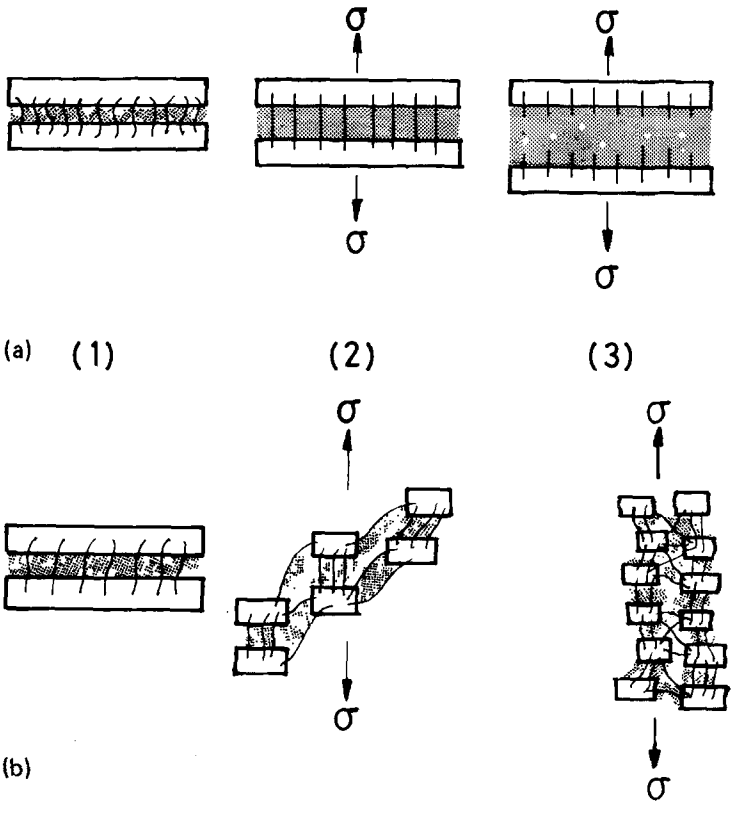

Figure 13 (a) Schematic diagram of fracturing of the LSC material: (1) unstrained strate; (2) prior to fracture; (3) interlamellar fracture. (b) Illustration of crystal fragmentation which produces necking upon yielding.

are no other estimates based on experimental observation other than those of the knife-cutting experiments of Backman and Devries. Our calculations indicate that tie molecules occupy only a small fraction of the non-crystalline region, unless it is assumed that there are defects in the specimens which produce stress concentrations greater than 50.

4.3.2. The D–B transitions of the LSC material

The unique D–B transitions in the LSC materials compared with all the other materials can now be understood. The LSC material has the greatest crystallinity and the least number of tie molecules. Therefore, just below its 260 K D–B transition the LSC material has the lowest fracture stress and a high yield point. When the LSC material is stressed the non-crystalline region deforms readily, giving the observed strain of about 0.10 and then the material fractures without fragmenting the crystals. If now the temperature is increased above 260 K into the α range, a weakening of the crystalline region begins. This weakening probably starts at the lamellar surface and progresses inwards. The weakening produces more and more strain prior to fracture without producing a catastrophic fragmentation of the crystals as occurs in the other materials. The fracture process may involve primarily the pulling out of the tie molecules at this temperature rather than chain rupture which predominates below 160 K. Besides the fact that the smaller number of tie molecules in the LSC material makes it more amenable to fracture, there is the additional possibility that crystal fragmentation does not occur readily because the number of tie molecules pulling on the crystals is less. The fracture process in the LSC material is illustrated in Fig. 13a where it can be compared with a schematic diagram of the localized necking that occurs via crystal fragmentation during yielding in the other materials (Fig. 13b). The micrograph in Fig. 14 shows the fissures in LSC after it has been fractured above the 200 K D–B transition. Figs. 14 and 1c suggest that there is little fragmentation of the crystals, but a form of ductile rupture occurs in the interlamellar region which is reminiscent of crazing as illustrated in Fig. 13a.

The effects of strain rate and temperature on the fracture strain of the LSC material as shown in Fig. 5 reflect the effects of the α-relaxation.

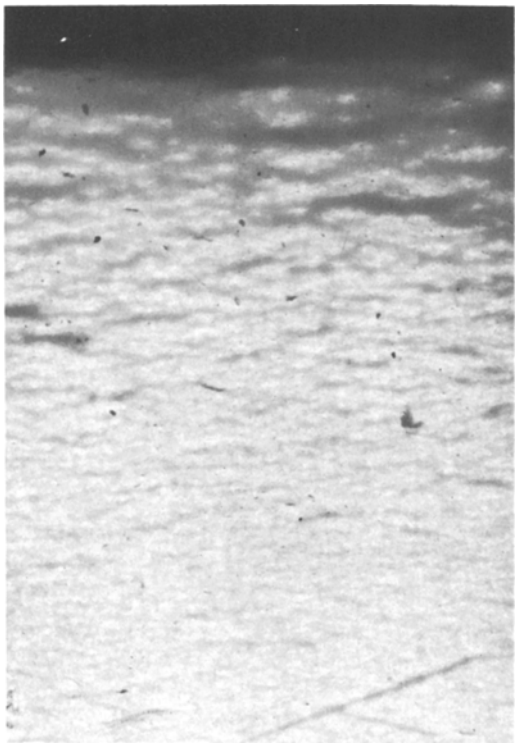

Figure 14 Optical micrograph of the LSC material fractured at 295 K. Note incipient cracks parallel to fracture surface at top (× 25).

The rapid increase in ϵ_F above 260 K may be associated with the weakening of the crystals due to the α-relaxation process.

The fracture strain, ϵ_F, below 260 K comes primarily from the non-crystalline region together with the elastic strain that occurs in the crystals. From 260 to 166 K ϵ_F is practically constant as little or no relaxation processes occur in this temperature range. Below 166 K, the γ-relaxation occurs so that the non-crystalline region becomes progressively more rigid and ϵ_F decreases. Below 130 K the γ-relaxations are quenched out so that ϵ_F becomes a purely elastic strain. Thus the 130 to 166 K D–B transition in LSC is attributed to the γ processes. Part of the decrease in ϵ_F below 166 K could come from γ-relaxations in the crystals.

4.4. Drawing and necking rupture

Whereas LSC fractures without crystal fragmentation at all temperatures below 300 K, the other materials form a neck and draw above 243 to 273 K and below this temperature range form a localized neck that leads to rupture. The neck formation is associated with a catastrophic fragmentation of the lamellar crystals as generally described by Peterlin [16], Peterman *et al.* [17], Haudin [15] and many others. In this investigation we are concerned with the transition from a stable neck and drawing to localized necking and rupture. The conditions for localized necking have been analysed by Coates and Ward [6]. They studied the effects of molecular weight and morphology on the necking and drawing behaviour of linear polyethylene at 21, 75 and 100° C. Their analysis is general and may be applied to all temperatures where plastic flow occurs.

Coates and Ward used an extension of the Considère analysis to describe the change in flow stress with strain. Four phenomena are involved: (1) the change in stress with cross-sectional area, the geometric effect; (2) the change in true stress with strain, the work hardening or orientation strengthening effect; (3) the change in stress with strain rate, the strain rate sensitivity; and (4) the change in stress with temperature, the effect of heating caused by plastic deformation. The effect of pressure could also be introduced, but it is not required for this analysis. The change in true stress is given by:

$$d\sigma = \left(\frac{\partial\sigma}{\partial\lambda}\right)_{\dot{\epsilon},T} d\lambda + \left(\frac{\partial\sigma}{\partial\dot{\epsilon}}\right)_{\lambda,T} d\dot{\epsilon} + \left(\frac{\partial\sigma}{\partial T}\right)_{\lambda,\dot{\epsilon}} dT.$$

Then

$$\frac{d\dot{\epsilon}}{d\lambda} = \left[\frac{d\sigma}{d\lambda} - \left(\frac{\partial\sigma}{\partial\lambda}\right)_{\dot{\epsilon},T} - \left(\frac{\partial\sigma}{\partial T}\right)_{\lambda,\dot{\epsilon}} \frac{dT}{d\lambda}\right]\left[\left(\frac{\partial\sigma}{\partial\dot{\epsilon}}\right)_{\lambda,T}\right]^{-1}.$$

$\dot{\epsilon}$, λ, σ, and T refer to the local value of the strain rate, strain, stress, and temperature. If $d\dot{\epsilon}/d\lambda$ is positive the strain rate increases locally with strain and localized necking occurs. If $d\dot{\epsilon}/d\lambda$ is negative the strain rate decreases leading to a stable neck and drawing would be expected.

The work-hardening factor $(\partial\sigma/\partial\lambda)_{\dot{\epsilon},T}$ is a positive quantity when orientation strengthening occurs, thus orientation strengthening tends to decrease $d\dot{\epsilon}/d\lambda$ and favours a stable neck. Coates and Ward found that $(\partial\sigma/\partial\lambda)_{\dot{\epsilon},T}$ increased with molecular weight. The change in $(\partial\sigma/\partial\lambda)_{\dot{\epsilon},T}$ with temperature is not known from this investigation, but it is expected to increase with decreasing temperature just as does the yield stress which is controlled by thermally activated processes. Thus if $(\partial\sigma/\partial\lambda)_{\dot{\epsilon},T}$ increased with decreasing temperature it would not explain why a localized necking occurs below 243 to 273 K.

It is suggested that the localized heating causes the localized necking. Since $(\partial\sigma/\partial T)_{\lambda,\dot{\epsilon}}$ is a negative quantity and $dT/d\lambda$, the temperature change generated by plastic deformation, is positive, localized necking is favoured. The rise in local temperature is related to the energy dissipated during yielding. This energy increases with the plastic work which, in turn, increases with the yield point or flow stress. Since the flow stress increases with decreasing temperature it is expected that the local rise in temperature may well increase with decreasing temperature for a given increment of plastic strain. Thus when the localized heating effect overcomes the work-hardening effect, localized necking is expected.

The strain rate sensitivity factor acts like a magnifying factor in that it controls the rate at which the neck stabilizes or localizes. The smaller $(\partial\sigma/d\dot{\epsilon})_{\lambda,T}$ the sharper the contour between necked and unnecked region. The LSC material exhibits a very shallow type of necking behaviour above 260 K so that it is expected to have a high strain rate sensitivity as also suggested previously by Coates and Ward [6].

4.5. Notch sensitivity

4.5.1. General discussion of notches

A notch concentrates the tensile stress, and the stress concentration $C = (1 + 2a/\rho)^{1/2}$ where a is the length of the notch perpendicular to the stress and ρ is its sharpness or radius of curvature [9]. If the notch is deformed by plastic deformation so that ρ increases, the effect of the notch decreases. In the case of an applied tensile stress, the notch perpendicular to the stress has a greater effect on the maximum normal stress which leads to fracture than on the maximum shear stress which leads to shear yielding. In addition, if a notch causes fracture, the crack propagates and increases the stress concentration of the notch. On the other hand, if a notch produces localized plastic deformation the material may be strengthened, reducing the effect of the notch. Furthermore, the plastic front then propagates away from the notch so that its effect becomes negligible in producing further plastic deformation. In summary, notches have a great effect on brittle fracture and a very much smaller effect on yielding. Thus brittle materials are notch sensitive and ductile materials much less so.

There are two quantitative ways of viewing the effect of a notch:

(1) fracture occurs when the local stress equals the intrinsic fracture stress of the material. We have

$$(1 + 2a/\rho)^{1/2}\,\sigma_f\,(\text{applied}) = \sigma_f\,(\text{ideal});$$

(2) the Griffith–Orowan–Irwin criterion based on energy considerations governing crack stability. This gives

$$\sigma_f(\text{applied})\,a^{1/2} = g\gamma(\text{material}),$$

where γ is the energy per unit area of fractured surface, a material parameter, and g is a constant based on specimen geometry. For sharp notches $a/\rho \gg 1$, and both criteria are identical. The energy criterion will still apply if a sufficiently small plastic zone forms in the vicinity of the notch tip as in the Dugdale model. The critical amount of plasticity which invalidates either of the above criteria is often a matter of uncertainty.

4.5.2. Comparison of the notch sensitivities of the LSC and LQ materials

Fig. 9 shows that the LQ material has about the same value of ultimate stress with or without a notch for temperatures down to about 130 K. Even at 100 K where the LQ material is completely brittle the ratio of the notched to unnotched strength is 0.88. The only effect of the notch above the D–B transition temperature of the LQ material is to produce a practically linear stress–strain curve instead of the typical ductile curve shown in Fig. 2. This means that the yield stress of the material governs the strength of the specimen and the notch stress concentration of the notch has little or no effect, presumably because the notch is blunted. A highly localized plastic deformation must occur at the tip of the notch which is followed by a localized rupture which then leads to fracture. Macroscopically, a large strain prior to fracture is not observed, because the localized plastic zone prior to rupture is small compared with the large plastic zone throughout the specimen cross-section prior to rupture in the unnotched specimen.

The LSC material shows considerable notch sensitivity at room temperature which increases with the decreasing temperature. This is to be expected since the ductility of the LSC material decreases with decreasing temperature. The interesting point is the comparison of the LQ and LSC materials in Fig. 10a and b where both materials in the unnotched state have the same ductility, but the LQ material shows little notch

sensitivity compared to the LSC material. If the notches were identical in both materials and both failed in a brittle manner, then they should both show the same ratio of $\sigma_f(N)/\sigma_f(U)$ according to the first criterion for failure given above. A possible explanation is that both materials do not have the same value of a/ρ which determines the stress concentration, because only the crack length a is controlled. The depth of inserting the razor blade to produce the notch was accurately controlled but ρ is unknown. It is likely that the LQ material, being more ductile at room temperature, has a larger value of ρ than the LSC material.

The difference in notch sensitivity between the LQ and LSC materials is not as readily explained by the energy criterion for failure. If we assume that there is an inherent crack in the unnotched material of length $a(U)$, then

$$\frac{\sigma_f(N)}{\sigma_f(U)} = \left[\frac{a(U)}{a(N)}\right]^{1/2}$$

Since $a(N)$ is the same for the LQ and LSC materials, and Fig. 10 shows that $\sigma_f(N)/\sigma_f(U)$ is greater for the LQ material than for the LSC material, it should follow that the inherent crack length in the LQ material is greater than in the LSC material. There is no reason for supposing that this is the case. Furthermore, since $\sigma_f(N)/\sigma_f(U)$ for the LQ material is about 0.88 in the brittle region, it means that the inherent crack length should be about 0.77 times the artificial crack length of 0.25 mm and this is not likely. A good expanation of this discrepancy is not at hand, and a resolution of the problem requires a more extensive investigation on the effects of notches with a wide range of lengths, also varying the method of producing the crack tip.

5. Conclusions

1. The brittle fracture stress of linear polyethylene increases with the number of tie molecules, and the number of tie molecules increases with molecular weight and the cooling rate from the melt.

2. The effect of morphology on the yield point becomes most prominent in a semi-crystalline polymer in the temperature range where the non-crystalline material is weakest and the crystals are strong. In this temperature range the crystallinity and the strength of the crystals control the yield point.

3. Below the γ-relaxation region the yield point is relatively insensitive to morphology, because the crystalline and non-crystalline regions have about the same strength.

4. Low molecular weight, slow cooled linear polyethylene material has unique fracture behaviour in that it is essentially brittle at all temperatures below about 260 K. This is because it has the lowest fracture stress and a high yield point.

5. The rapid increase in ductility of the slow cooled low molecular weight linear polyethylene material above about 260 K is associated with softening of the crystals due to the α-relaxation.

6. Slow cooled low molecular weight material is very notch sensitive compared with quenched material which is not notch sensitive even in its brittle range for notches about 0.25 mm deep.

7. The transition from necking and drawing behaviour to localized necking and rupture behaviour below about 243 to 273 K for quenched and high molecular weight materials is mostly caused by the localized heating produced during necking at the yield point.

Acknowledgements

We wish to thank Mr D. L. M. Cansfield and Mr J. Defty for assistance with experimental work. The Gas Research Institute gave support to NB. This work was done while NB was on sabbatical leave at the University of Leeds.

References

1. M. K. V. CHAN and J. G. WILLIAMS, *Polym. Eng. Sci.* **21** (1981) 1026.
2. R. W. TRUSS, R. A. DUCKETT and I. M. WARD, *J. Mater. Sci.* **16** (1981) 1689.
3. G. CAPACCIO and I. M. WARD, *Polymer* **15** (1974) 233.
4. *Idem, ibid.* **16** (1975) 239.
5. G. CAPACCIO. T. A. CROMPTON and I. M. WARD, *J. Polymer Sci. Polymer Phys. Ed.* **14** (1976) 1641.
6. P. D. COATES and I. M. WARD, *J. Mater. Sci.* **15** (1980) 2897.
7. G. CAPACCIO, I. M. WARD, M. A. WILDING and G. W. LONGMAN, *J. Macromol. Sci. Phys.* **B15** (1978) 381.
8. N. BROWN and M. PARRISH, *J. Polymer Sci. Polymer Lett. Ed.* **10** (1972) 777.
9. I. M. WARD, "Mechanical Properties of Polymers", 1st edn (Wiley, London, 1971).
10. J. R. KASTELIC and E. BAER, *J. Macromol. Sci. Phys.* **B7** (1973) 679.
11. D. C. BASSETT and A. M. HODGE, *Proc. Roy. Soc. London* **A377** (1981) 25.
12. D. C. BASSETT, A. M. HODGE and R. H. OLLEY, *Faraday Discuss. Chem. Soc.* **68** (1979) 218.

13. J. DLUGOSZ, G. V. FRASER, D. GRUBB, A. KELLER, J. A. ODELL and P. L. GOGGIN, *Polymer* **17** (1976) 471.
14. D. K. BACKMAN and K. L. DEVRIES, *J. Polymer Sci.* **A1 7** (1969) 2125.
15. J. M. HAUDIN, "Plastic Deformation of Semi-crystalline Polymers" Spring School on Plastic Deformation of Polymers, Les Houches, April (1982).
16. A. PETERLIN, *Kolloid Z.u. Polymere* **233** (1969) 857.
17. J. PETERMAN, W. KLUGE and H. GLEITER, *J. Polymer Sci. Polymer Phys. Ed.* **17** (1979) 1043.
18. E. KAMEI and N. BROWN, private communication on research at University of Pennsylvania (1982).
19. A. KELLY, "Strong Solids", 2nd edn (Clarendon Press, Oxford, 1973) p. 10.
20. I. M. WARD (ed.) "Advances in Oriented Polymers 1" (Applied Science Publishers, London, 1982) Ch. 5.

Received 8 September
and accepted 6 October 1982